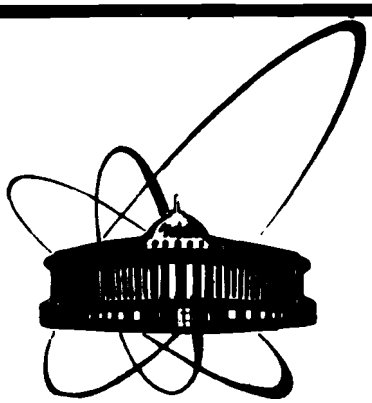

объединенный
институт
ядерных
исследований
дубна

E4-88-158

R.Kuchta

MICROSCOPIC MEAN-FIELD BOSON APPROACH TO THE SHAPE TRANSITION IN Sm ISOTOPES

Submitted to "Nuclear Physics A"

1988

1. Introduction

A theoretical treatment of the transition from vibrational to rotational spectra in the chain of Sm isotopes provides a good test for the adequacy of various nuclear models. At the phenomenological level, a great success has been achieved in the framework of the interacting boson model (IBM) [ref. [1]]. At the microscopic level, however, the situation appears to be much more complicated. The microscopic approaches dealing with this problem [2,3] generally start from the shell model in the quasiparticle representation, truncate the fermion basis so as to include only quadrupole ($J=2$) two-quasiparticle excitations (both the collective and the non-collective ones) and map the truncated fermion problem onto the boson space using the boson expansion technique [4]. The work of Kishimoto and Tamura [2] makes use of the Holstein-Primakoff boson mapping [5] which represents the original fermion hamiltonian as an infinite series in the boson operators. Convergence of this series is sufficiently fast when only the collective quadrupole bosons are retained [6] but it is much slower if the non-collective bosons are taken into account [7]. Since the non-collective bosons were found [2] to play an important role just in the transitional region, the inclusion of the higher-order boson interactions in the hamiltonian turns out to be inevitable. In order to avoid this difficulty, Tsukuma, Thorn and Takada (TTT) have proposed [3] to use the Dyson mapping [8] which is free from the problem of convergence. Applications of the Dyson mapping have long been impeded by the fact that the mapping is non-unitary and thus leads to a non-her-

mitian boson hamiltonian. Today, however, this problem is completely solved[7], and therefore, one can fully exploit the finiteness of the Dyson boson expansion. Nevertheless, in spite of all the advantages and a great utility of the Dyson mapping in the description of nuclear properties [9-12], TTT [ref. 3)] were unable to reproduce the shape transition from the spherical (vibrational) nuclei to the deformed (rotational) ones in the chain of Sm isotopes.

The purpose of the present paper is to show that the failure of the TTT approach can most likely be attributed to the neglect of the higher-multipole ($J > 2$) bosons. In fact, it is well known[13] that a satisfactory microscopic description of the low-lying states in deformed nuclei requires an explicit inclusion of at least the $J = 4$ bosons, corresponding to the $J = 4$ fermion pairs. We use the Dyson mapping here as TTT did in ref.[3]), but we apply it directly to the shell-model hamiltonian without performing the quasiparticle transformation. Instead of restricting in advance the fermion space to the subspace of quadrupole ($J = 2$) pairs, we first map the entire fermion space onto a boson one and than apply an appropriate variational principle to the mapped boson hamiltonian. This procedure enables us to take into account the bosons with all admissible angular momenta. As will be seen, there is a considerable increase in the percentage of J=4 bosons in the variational wave function at A = 152 (A is the mass number of a nucleus) and it is just this fact that leads to a good reproduction of the shape transition from the spherical to the deformed region.

The paper is arranged as follows. In sect. 2 we give an outline of the method. Sect. 3 contains our numerical results and their comparison with experiment as well as with the results of other approaches, namely the phenomenological IBM [ref.[14])] and the microscopic TTT [ref. 3)]. Conclusions from our investigations are collected in sect. 4.

2. Outline of the method

2.1. BOSON IMAGE OF THE SHELL-MODEL HAMILTONIAN

We start from the description of a heavy nucleus as a system of n_π valence protons and n_ν valence neutrons distributed over different shell-model orbitals. We confine our discussion to even-even nuclei only. The associated shell-model hamiltonian can be written as a sum of a hamiltonian for protons and neutrons separately plus a term describing an interaction between protons and neutrons:

$$H = H(\pi) + H(\nu) + V(\pi\nu) \,, \tag{2.1}$$

where τ (ν) designates proton (neutron). The hamiltonian for identical nucleons is taken to have the form

$$H(\rho) = \sum_{\rho_1} \varepsilon_{\rho_1} c^\dagger_{\rho_1} c_{\rho_1} + \frac{1}{4} \sum_{\rho_1\rho_2\rho_3\rho_4} G_{\rho_1\rho_2\rho_3\rho_4}\, c^\dagger_{\rho_1} c^\dagger_{\rho_2} c_{\rho_4} c_{\rho_3} + \frac{1}{2} \sum_{\rho_1\rho_2\rho_3\rho_4} F_{\rho_1\rho_3\rho_2\rho_4}\, c^\dagger_{\rho_1} c_{\rho_2} c^\dagger_{\rho_3} c_{\rho_4} \,, \tag{2.2}$$

where ρ is either τ or ν, the indices ρ_i completely specify the shell-model single-particle states, $\rho_i = (n^\rho_i, l^\rho_i, j^\rho_i, m^\rho_i)$, $c^\dagger_{\rho_i}$ (c_{ρ_i}) are the creation (annihilation) operators for nucleons in these states, ε_{ρ_i} are the corresponding single-particle energies and $G_{\rho_1\rho_2\rho_3\rho_4}$, $F_{\rho_1\rho_3\rho_2\rho_4}$ are matrix elements of an effective nucleon-nucleon interaction. We assume that the interaction $G_{\rho_1\rho_2\rho_3\rho_4}$ is coherent in the particle-particle channel and is antisymmetrized, while $F_{\rho_1\rho_3\rho_2\rho_4}$ is coherent in the particle-hole channel and is not antisymmetrized. A special type of this interaction is the $P_0 + P_2 + QQ$ force which has been used by TTT in ref.[3]) and which will be employed in the present calculation as well. The last term $V(\pi\nu)$ in (2.1) represents the proton-neutron interaction and is given by

$$V(\pi\nu) = \frac{1}{2} \sum_{\substack{\pi_1\pi_2\\ \nu_1\nu_2}} V_{\pi_1\nu_1\pi_2\nu_2}\, c^\dagger_{\pi_1} c_{\pi_2} c^\dagger_{\nu_1} c_{\nu_2} \,. \tag{2.3}$$

All the interactions involved in (2.1) are supposed to have the usual hermitian and time reversal properties.

For the purpose of analyzing the original fermion problem in the boson space, one introduces the ideal boson creation and annihilation operators $b^+_{\rho_1\rho_2}$, $b_{\rho_1\rho_2}$ which satisfy the following antisymmetry and commutation relations

$$b^+_{\rho_1\rho_2} = - b^+_{\rho_2\rho_1} \quad , \qquad (2.4a)$$

$$\begin{aligned} &[b_{\rho_1\rho_2}, b_{\rho_3\rho_4}] = [b^+_{\rho_1\rho_2}, b^+_{\rho_3\rho_4}] = 0 \\ &[b_{\rho_1\rho_2}, b^+_{\rho_3\rho_4}] = \delta_{\rho_1\rho_3}\delta_{\rho_2\rho_4} - \delta_{\rho_1\rho_4}\delta_{\rho_2\rho_3} \\ &[b_{\rho_1\rho_2}, b^+_{\rho'_3\rho'_4}] = [b_{\rho_1\rho_2}, b_{\rho'_3\rho'_4}] = [b^+_{\rho_1\rho_2}, b^+_{\rho'_3\rho'_4}] = 0 \ , \end{aligned} \qquad (2.4b)$$

where $\rho' = \nu$ if $\rho = \pi$ and $\rho' = \pi$ if $\rho = \nu$. We do not consider the $b^+_{\pi\nu}$ - bosons here since there is no indication for their importance in heavy nuclei, where protons and neutrons occupy very different single-particle orbitals [15]. The whole ideal boson space is spanned by the many-boson states of the form

$$\prod_{\rho=\pi,\nu} b^+_{\rho_1\rho_2} b^+_{\rho_3\rho_4} \cdots b^+_{\rho_{N-1}\rho_N} |0)_B \ ,$$

where $|0)_B$ is the boson vacuum, $b_{\rho_1\rho_2}|0)_B = 0$. Those states which properly take into account the Pauli principle and thus are in one-to-one correspondence with the fermion states, define the so-called physical boson subspace [16,17]. It is this subspace in which the actual calculations have to be carried out in order to avoid spurious solutions [17,18].

As is well known [4,17], it is possible to construct a finite boson realization of the algebra generated by the bifermion operators $c^+_{\rho_1}c^+_{\rho_2}$, $c_{\rho_1}c_{\rho_2}$, $c^+_{\rho_1}c_{\rho_2}$ in terms of the boson operators $b^+_{\rho_1\rho_2}, b_{\rho_3\rho_4}$. This is the famous non-unitary mapping introduced by Dyson [8]

$$c^+_{\rho_1}c^+_{\rho_2} \to \mathcal{B}^+_{\rho_1\rho_2} = b^+_{\rho_1\rho_2} - \sum_{\rho_3\rho_4} b^+_{\rho_1\rho_3} b^+_{\rho_2\rho_4} b_{\rho_3\rho_4} \ , \qquad (2.5a)$$

$$c_{\rho_1}c_{\rho_2} \to b_{\rho_2\rho_1} \ , \qquad (2.5b)$$

$$c^+_{\rho_1}c_{\rho_2} \to \sum_{\rho_3} b^+_{\rho_1\rho_3} b_{\rho_2\rho_3} \ . \qquad (2.5c)$$

In recent years, the theory based on eqs. (2.5) has proved to yield a powerful method for investigating nuclear collective motion [9-12]. With the help of (2.2), (2.3) and (2.5) we can easily find an exact non-hermitian boson image of the shell-model hamiltonian (2.1) and treat it within an appropriate hermitization procedure [9]. Alternatively, we can rearrange the identical nucleon hamiltonian (2.2) into the form

$$H(\rho) = \sum_{\rho_1\rho_2} \left(\varepsilon_{\rho_1}\delta_{\rho_1\rho_2} + \tfrac{1}{4}\sum_{\rho_3} G_{\rho_1\rho_3\rho_2\rho_3}\right) c^+_{\rho_1}c_{\rho_2} + \tfrac{1}{4}\sum_{\substack{\rho_1\rho_2\\ \rho_3\rho_4}} W_{\rho_1\rho_3\rho_2\rho_4}\, c^+_{\rho_1}c^+_{\rho_3}c_{\rho_4}c_{\rho_2} \ , \qquad (2.6)$$

where

$$W_{\rho_1\rho_3\rho_2\rho_4} = G_{\rho_1\rho_3\rho_2\rho_4} + 2\, F_{\rho_1\rho_3\rho_2\rho_4} \ , \qquad (2.7)$$

and use only the mapping (2.5c) for the c^+c -type operators. Both versions of the bosonization procedure are completely equivalent [19] but the latter provides directly a hermitian boson hamiltonian, so that the additional hermitization procedure can be avoided. Using (2.6), (2.3) and (2.5c), the hermitian Dyson boson image of the original shell-model hamiltonian (2.1) can be written (in the normal ordered form with respect to the boson vacuum $|0)_B$) as

$$H_B = H_B(\pi) + H_B(\nu) + V_B(\pi\nu) \ , \qquad (2.8)$$

where

$$H_B(\rho) = {}^{(1)}H^0_B(\rho) + {}^{(2)}H^0_B(\rho) + H^{int}_B(\rho) \ , \qquad (2.9a)$$

$${}^{(1)}H^0_B(\rho) = \sum_{\rho_1\rho_2\rho_3} \left(\varepsilon_{\rho_1}\delta_{\rho_1\rho_2} + \tfrac{1}{2}\sum_{\rho_4} F_{\rho_1\rho_4\rho_3\rho_2}\right) b^+_{\rho_1\rho_3} b_{\rho_2\rho_3} \ , \qquad (2.9b)$$

$${}^{(2)}H^0_B(\rho) = \tfrac{1}{4}\sum_{\rho_1\rho_2\rho_3\rho_4} W_{\rho_1\rho_2\rho_3\rho_4}\, b^+_{\rho_1\rho_2} b_{\rho_3\rho_4} \ , \qquad (2.9c)$$

$$H^{int}_B(\rho) = \tfrac{1}{4}\sum_{\substack{\rho_1\rho_2\rho_3\rho_4\\ \rho_5\rho_6}} W_{\rho_1\rho_2\rho_3\rho_4}\, b^+_{\rho_1\rho_5} b^+_{\rho_4\rho_6} b_{\rho_3\rho_5} b_{\rho_2\rho_6} \ , \qquad (2.9d)$$

$\rho = \pi, \nu$;

$$V_B(\pi\nu) = \tfrac{1}{2}\sum_{\substack{\pi_1\pi_2\pi_3\\ \nu_1\nu_2\nu_3}} V_{\pi_1\nu_1\pi_2\nu_2}\, b^+_{\pi_1\pi_3} b^+_{\nu_1\nu_3} b_{\pi_2\pi_3} b_{\nu_2\nu_3} \ . \qquad (2.10)$$

It should be emphasized that a hermitian Dyson hamiltonian with at most two-body boson terms (which is in fact also the Holstein - Primakoff image) has been obtained due to the fact that the mapping was applied directly to the original shell-model hamiltonian and not to its quasiparticle representation. As is well known [4], the latter produces a number-non-conserving fermion hamiltonian, which always leads either to the non-hermitian Dyson image with up to three-body boson terms or to the hermitian Holstein - Primakoff image represented by an infinite series in the boson operators. It is also worth remarking that the present form of the boson hamiltonian commutes with the projection operator onto the physical boson subspace [20], which is not the case when working in the quasiparticle representation [6].

2.2. PHYSICAL BOSON STATES

As already mentioned, any calculation in the boson space is relevant to the underlying fermion problem only when it is carried out in the physical boson subspace in which every boson state has its fermion counterpart. It was originally shown by Janssen et al.[17] and later elaborated by Li[21] and Park[20] that a normalized physical N_ρ-boson state $|N_\rho; \rho^{h\gamma^s}\rangle_B$ had to satisfy the condition

$$ {}_B\langle N_\rho; \rho^{h\gamma^s} | \hat{S}_B(\rho) | N_\rho; \rho^{h\gamma^s}\rangle_B = 2N_\rho(2N_\rho - 1) , \qquad (2.11) $$

where

$$ \hat{S}_B(\rho) = \sum_{\rho_1\rho_2} \mathcal{B}^+_{\rho_1\rho_2} b_{\rho_1\rho_2} = \sum_{\rho_1\rho_2} b^+_{\rho_1\rho_2} b_{\rho_1\rho_2} - \sum_{\rho_1\rho_2\rho_3\rho_4} b^+_{\rho_1\rho_3} b^+_{\rho_2\rho_4} b_{\rho_3\rho_1} b_{\rho_4\rho_2} \qquad (2.12) $$

and ρ is either π or ν. The operator $\hat{S}_B(\rho)$ is nothing but the Dyson boson image of the fermion operator

$$ \hat{S}(\rho) = \hat{n}_\rho(\hat{n}_\rho - 1) ; \qquad \hat{n}_\rho = \sum_{\rho_1} c^+_{\rho_1} c_{\rho_1} , \qquad (2.13) $$

written in the normal-ordered form

$$ \hat{S}(\rho) = \sum_{\rho_1\rho_2} c^+_{\rho_1} c^+_{\rho_2} c_{\rho_2} c_{\rho_1} . \qquad (2.14) $$

As before, $\hat{S}_B(\rho)$ is also the Holstein-Primakoff image of $\hat{S}(\rho)$. Realizing that $n_\rho = 2N_\rho$ and the operator $\hat{S}_B(\rho)$ antisymmetrizes the indices belonging to different bosons in a many-boson state, the condition (2.11) can easily be understood as the requirement that the state $|N_\rho; \rho^{h\gamma^s}\rangle_B$ is completely antisymmetrized in all the boson indices, and consequently, it satisfies the Pauli principle for fermions. In the following we will restrict our discussion to the states $|N_\rho; \rho^{h\gamma^s}\rangle_B$ only.

2.3. THE MEAN-FIELD APPROXIMATION

The diagonalization of the boson hamiltonian (2.8) in the physical boson basis is completely equivalent to the full shell-model calculation and hence impracticable in general cases. An application to real nuclei thus requires an adequate approximation which consists in truncating the basis to a small set of collective degrees of freedom. How to perform this truncation is the crucial problem which lies at the very heart of the microscopic theory of nuclear collective motion. Various approaches have been suggested to deal with this problem[22-24]. Their common feature is that they are based (in one or another way) on the mean-field approximation (MFA)[4]. The basic idea behind the MFA is to apply an appropriate variational principle to the hamiltonian in order to get the ground state of the system considered (the Hartree approximation - HA) and then to generate the lowest excited states in the framework of the Tamm-Dancoff approximation (TDA) or the random phase approximation (RPA). The variational procedure can be applied either to the fermion hamiltonian[22,23] or to the boson one[22,21,24]. Both the phenomenological[24] and the microscopically derived[22,21] boson hamiltonians have been used. Working with the latter, however, an explicit restriction of the variational space to the physical boson subspace seems to be

important[21,25], although in some special cases (e.g. not-too-large numbers of bosons or/and a specific interaction) the neglect of the Pauli principle in the boson space still leads to reasonable results[12].

In this work, we apply the MFA to the mapped boson hamiltonian (2.8) and the Pauli principle is taken into account through the condition (2.11). We assume that the boson ground-state (GS) wave function has the form

$$|GS;N_\pi,N_\nu\rangle_B = \frac{1}{\sqrt{N_\pi!\,N_\nu!}}\left(B_0^+(\pi)\right)^{N_\pi}\left(B_0^+(\nu)\right)^{N_\nu}|0\rangle_B , \qquad (2.15)$$

where N_ρ ($\rho=\pi,\nu$) is half the number of valence nucleons of type ρ ($N_\rho=\frac{n_\rho}{2}$) and

$$B_0^+(\rho) = \frac{1}{\sqrt{2}}\sum_{\rho_1\rho_2} X^0_{\rho_1\rho_2} b^+_{\rho_1\rho_2} . \qquad (2.16)$$

The particular collective bosons (2.16), hereafter referred to as the Hartree bosons, are specified in terms of the coefficients $X^0_{\rho_1\rho_2}$ which are regarded as variational parameters and determined by minimizing the expectation value of the hamiltonian (2.8) in the state (2.15) under the restrictions

$$\left[B_0(\rho),\,B_0^+(\rho')\right] = \delta_{\rho\rho'} , \qquad (2.17)$$

$$_B\langle GS;N_\pi,N_\nu|\hat{S}_B(\rho)|GS;N_\pi,N_\nu\rangle_B = 2N_\rho(2N_\rho-1) , \qquad (2.18)$$

where $\hat{S}_B(\rho)$ is given by (2.12). In order to reduce the number of independent variational parameters, we impose on $X^0_{\rho_1\rho_2}$ the following symmetry requirements:

$$X^0_{\rho_1\rho_2} = -X^0_{\rho_2\rho_1} , \qquad (2.19)$$

$$X^0_{\rho_1\rho_2} = \eta_{\rho_1}\eta_{\rho_2}X^0_{\bar{\rho}_1\bar{\rho}_2} \;;\; \eta_{\rho i}=(-)^{j^\rho_i-m^\rho_i} ,\; \bar{\rho}_i=(n^\rho_i,l^\rho_i,j^\rho_i,-m^\rho_i) \qquad (2.20)$$

$$X^0_{\rho_1\rho_2} = \delta_{m^\rho_1,-m^\rho_2}\cdot X^0_{\rho_1\rho_2} . \qquad (2.21)$$

Eq. (2.19) reflects the Pauli principle for the one-boson states [see (2.4a)], the condition (2.20) expresses time reversal invariance and (2.21) restricts the ground state (2.15) to be axially symmetric (K = 0).

The restricted variational calculation leads to the standard non-linear eigenvalue problem[24]. The eigenvector corresponding to the lowest eigenvalue yields the amplitudes $X^0_{\rho_1\rho_2}$ which define the Hartree bosons (2.16) and thus the boson ground state (2.15). The remaining eigenvectors, associated with higher eigenvalues, provide a set of "excited" bosons $B^+_\alpha(\rho)$ orthogonal to $B^+_0(\rho)$,

$$B^+_\alpha(\rho) = \frac{1}{\sqrt{2}}\sum_{\rho_1\rho_2} X^\alpha_{\rho_1\rho_2} b^+_{\rho_1\rho_2} ,$$
$$\sum_{\rho_1\rho_2} X^\alpha_{\rho_1\rho_2} X^0_{\rho_1\rho_2} = 0 . \qquad (2.22)$$

In terms of $B^+_\alpha(\rho)$, we can define the following one-boson excitations of the condensate (2.15):

$$|\alpha,\pi;N_\pi,N_\nu\rangle_B = B^+_\alpha(\pi)|GS;N_\pi-1,N_\nu\rangle_B ,$$
$$|\alpha,\nu;N_\pi,N_\nu\rangle_B = B^+_\alpha(\nu)|GS;N_\pi,N_\nu-1\rangle_B . \qquad (2.23)$$

The states (2.23) form the TDA basis for diagonalizing the Dyson hamiltonian $\hat{H}_B$. The resulting eigenvectors can be written as

$$|i;N_\pi,N_\nu\rangle_B = \sum_\alpha X^i_\alpha(\pi)|\alpha,\pi;N_\pi,N_\nu\rangle_B + \sum_\alpha X^i_\alpha(\nu)|\alpha,\nu;N_\pi,N_\nu\rangle_B \qquad (2.24)$$

and they describe the excited K = 0 states ($i=1,2,\ldots$) of the system under consideration within the bosonic TDA.

Before proceeding further, a remark about the physical character of the boson states (2.24) is in order. Since the amplitudes $X^\alpha_{\rho_1\rho_2}$ are solutions of the same equations as $X^0_{\rho_1\rho_2}$, they satisfy the condition (2.11), implying that the TDA basis (2.23) is physical. As mentioned at the end of the subsect. 2.1., the present form of the Dyson hamiltonian $\hat{H}_B$ commutes with the projector onto the physical boson subspace. Consequently, the diagonalization of $\hat{H}_B$ in the physical basis (2.23) has to produce physical eigenstates.

2.4. ANGULAR MOMENTUM STRUCTURE OF THE MF BOSON STATES

In accordance with the structure of the boson hamiltonian [see eqs. (2.8) - (2.10)], we can define a set of one-boson eigenstates of $\hat{H}_B$ with a definite angular momentum JM,

$$\hat{H}_B\, b^+_{JM\sigma}(\rho)|0\rangle_B = E_{\sigma J}(\rho)\, b^+_{JM\sigma}(\rho)|0\rangle_B \,, \qquad (2.25)$$

$$b^+_{JM\sigma}(\rho) = \frac{1}{\sqrt{2}} \sum_{\rho_1\rho_2} \psi^{J\sigma}_{12}(\rho) \langle j_1 m_1 j_2 m_2 | JM\rangle b^+_{\rho_1\rho_2} \,, \qquad (2.26)$$

$1 \equiv (n^\rho_1, l^\rho_1, j^\rho_1)$, $\rho_1 = (1, m^\rho_1)$,

where $\langle j_1 m_1 j_2 m_2 | JM\rangle$ is the usual Clebsch-Gordan coefficient and the index σ with values 0,1,2,... distinguishes between bosons with the same JM so that the energy $E_{\sigma J}(\rho)$ increases with σ. In terms of the $b^+_{JM\sigma}(\rho)$ - operators one can express the mean-field (MF) bosons $B^+_\alpha(\rho)$ $(\alpha = 0,\alpha)$ as

$$B^+_\alpha(\rho) = \sum_{JM\sigma} u^\alpha_{JM\sigma}(\rho)\, b^+_{JM\sigma}(\rho) \,, \qquad (2.27)$$

where

$$u^\alpha_{JM\sigma}(\rho) = \sum_{\rho_1\rho_2} \psi^{J\sigma}_{12}(\rho)\, X^\alpha_{\rho_1\rho_2} \langle j^\rho_1 m^\rho_1 j^\rho_2 m^\rho_2 | JM\rangle \,; \quad \alpha = 0,\alpha \,. \qquad (2.28)$$

Making use of the relations (2.19) - (2.21) and exploiting the symmetry properties of the Clebsh-Gordan coefficients, it is easy to see that only the amplitudes $u^\alpha_{J0\sigma}(\rho)$ with even J are present in the expansion (2.27).

The MF boson states (2.15) and (2.24) can be viewed as intrinsic states from which the ones with definite angular momenta are obtained by projecting out the desired component,

$$|\omega; JM\rangle_B = \mathcal{N}^\rho_{\omega J}\, \hat{P}^J_{M0}\, |\omega; N_\pi, N_\nu\rangle_B \,; \quad \omega = GS, i \,, \qquad (2.29)$$

where $\mathcal{N}^\rho_{\omega J}$ is the normalization constant and

$$\hat{P}^J_{MK} = \frac{2J+1}{8\pi^2} \int D^{J*}_{MK}(\Omega)\, \hat{R}(\Omega)\, d\Omega$$

is the angular momentum projection operator [4] .

The excitation energies of the states (2.29) are then simply given by

$$E_{J\omega} = {}_B\langle \omega; JM|\, \hat{H}_B\, |\omega; JM\rangle_B - \langle GS;00|\, \hat{H}_B\, |GS;00\rangle_B \,. \qquad (2.30)$$

2.5. TRANSITION OPERATORS

The proper theoretical treatment of electromagnetic transitions in nuclei is traditionally considered to provide a powerful tool for our understanding of nuclear properties. In particular, the analysis of electron scattering from nuclei supplies valuable and detailed information on the structure of nuclear states [26,27] . In this paper we will confine ourselves to the Eλ transitions. The associated transition operators are written as

$$\hat{T}_{\lambda\mu}(r) = \hat{T}^\pi_{\lambda\mu}(r) + \hat{T}^\nu_{\lambda\mu}(r) \,,$$
$$\hat{T}^\rho_{\lambda\mu}(r) = e^\rho_{eff} \sum_{\rho_1\rho_2} \phi^*_{\rho_1}(r)\phi_{\rho_2}(r) \langle \rho_1|Y_{\lambda\mu}|\rho_2\rangle\, c^+_{\rho_1} c_{\rho_2} \,, \quad \rho = \pi,\nu \qquad (2.31)$$

where e^ρ_{eff} is the nucleon effective charge, $\phi_{\rho_i}(r)$ stands for the radial part of the nucleon single-particle wave function and $Y_{\lambda\mu}$ are the usual spherical harmonics. The boson image $\hat{T}^B_{\lambda\mu}(r)$ of $\hat{T}_{\lambda\mu}(r)$ is obtained through the replacement of the fermion operator $c^+_{\rho_1} c_{\rho_2}$ in (2.31) by its boson counterpart according to (2.5c) . The transition density of multipolarity λ from an initial nuclear state $|i\rangle$ to the final one $|f\rangle$ can then be expressed as

$$\rho^{i\to f}_\lambda(r) = {}_B\langle \omega_f;\, J_f \|\, \hat{T}^B_\lambda(r)\, \|\, \omega_i;\, J_i\rangle_B \,, \qquad (2.32)$$

where the symbol $\langle .. \| \| .. \rangle$ denotes the reduced matrix element and the boson states $|\omega_i; J_i M_i\rangle_B$, $|\omega_f; J_f M_f\rangle_B$ are defined by eq. (2.29) . The transition densities (2.32) are assumed to be normalized so that

$$B(E\lambda;\, i\to f) = \left| \int_0^\infty \rho^{i\to f}_\lambda(r)\, r^{\lambda+2}\, dr \right|^2 . \qquad (2.33)$$

3. Application to $^{146-156}$Sm.

3.1. SHELL-MODEL SPACE AND INTERACTION

We have applied the mean-field boson approach, described in the previous section, to the Sm isotopes in order to see whether it is able to account for the characteristic changes in the energy spectra and Eλ transitions when moving from ^{146}Sm towards ^{156}Sm. The active single-particle orbits were chosen to be $1g_{7/2}$, $1g_{9/2}$, $2d_{5/2}$, $1h_{11/2}$, $2d_{3/2}$, $3s_{1/2}$, $1h_{9/2}$, $2f_{7/2}$ for protons and $1h_{11/2}$, $1h_{9/2}$, $2f_{7/2}$, $1i_{13/2}$, $3p_{3/2}$, $2f_{5/2}$, $3p_{1/2}$, $1i_{13/2}$, $2g_{9/2}$ for neutrons. Their energies were taken from ref. [18]. The associated single-particle wave functions were assumed to be the harmonic-oscillator ones with the oscillator parameter $b = 1.0\ A^{1/6}$ fm (A is the mass number of a nucleus). With the above choice of single-particle orbits there are 40 inactive protons and 70 inactive neutrons, so that for $^{146-156}_{62}$Sm one has $n_\pi = 22$ valence protons and $n_\nu = 14 - 24$ valence neutrons. The corresponding boson numbers N_π and N_ν, appearing in (2.15), are therefore equal to 11 and 7 - 12, respectively.

The proton-proton and neutron-neutron interaction used in the present work consists of the monopole pairing (P_0), the quadrupole pairing (P_2) and the quadrupole-quadrupole (QQ) force,

$$V(\rho\rho) = -\tfrac{1}{4} G_0(\rho) \hat{P}^\dagger_{00}(\rho) \hat{P}_{00}(\rho) - \tfrac{1}{2} G_2(\rho) \sum_M \hat{P}^\dagger_{2M}(\rho) \hat{P}_{2M}(\rho) - \tfrac{1}{2} \kappa_\rho \sum_M \hat{Q}^\dagger_{2M}(\rho) \hat{Q}_{2M}(\rho) \; ; \quad \rho = \pi, \nu \;, \tag{3.1}$$

while the proton-neutron interaction is assumed to be represented by the pure quadrupole-quadrupole (QQ) force,

$$V(\pi\nu) = -\tfrac{1}{2} \kappa_{\pi\nu} \sum_M \hat{Q}^\dagger_{2M}(\pi) \hat{Q}_{2M}(\nu) \;. \tag{3.2}$$

The numbers $G_0(\rho)$, $G_2(\rho)$, κ_ρ, $\kappa_{\pi\nu}$ are the respective strength parameters and the operators $\hat{P}^\dagger_{00}(\rho)$, $\hat{P}^\dagger_{2M}(\rho)$, $\hat{Q}^\dagger_{2M}(\rho)$ are defined through

$$\hat{P}^\dagger_{00}(\rho) = \sum_{\rho_1} \eta_{\rho_1} c^\dagger_{\rho_1} c^\dagger_{\bar{\rho}_1} \;, \tag{3.3}$$

$$\hat{P}^\dagger_{2M}(\rho) = \sum_{\rho_1 \rho_2} \langle \rho_1 | r^2 Y_{2M} | \rho_2 \rangle \eta_{\rho_2} c^\dagger_{\rho_1} c^\dagger_{\bar{\rho}_2} \;, \tag{3.4}$$

$$Q^\dagger_{2M}(\rho) = \sum_{\rho_1 \rho_2} \langle \rho_1 | r^2 Y_{2M} | \rho_2 \rangle \, c^\dagger_{\rho_1} c_{\rho_2} \tag{3.5}$$

with η_{ρ_i}, $\bar{\rho}_i$ specified in (2.20). The interaction (3.1) corresponds to the matrix elements

$$G_{\rho_1\rho_2\rho_3\rho_4} = -G_0(\rho) \eta_{\rho_1} \eta_{\rho_3} \delta_{\rho_1\bar{\rho}_2} \delta_{\rho_3\bar{\rho}_4} - 2 G_2(\rho) \sum_M \eta_{\rho_2} \eta_{\rho_4} \langle \rho_1 | r^2 Y_{2M} | \bar{\rho}_2 \rangle \langle \rho_3 | r^2 Y_{2M} | \bar{\rho}_4 \rangle \;,$$

$$F_{\rho_1\rho_2\rho_3\rho_4} = -\kappa_\rho \sum_M \langle \rho_1 | r^2 Y_{2M} | \rho_2 \rangle \langle \rho_3 | r^2 Y_{2M} | \rho_4 \rangle \;, \tag{3.6}$$

appearing in the hamiltonian (2.2). Similarly, the interaction (3.2) yields

$$V_{\pi_1\nu_1\pi_2\nu_2} = -\kappa_{\pi\nu} \sum_M \langle \pi_1 | r^2 Y_{2M} | \pi_2 \rangle \langle \nu_1 | r^2 Y_{2M} | \nu_2 \rangle \tag{3.7}$$

[see eq. (2.3)]. The strengths $G_0(\rho)$, $G_2(\rho)$, κ_ρ and $\kappa_{\pi\nu}$ are taken to be [18,3]

$$G_0(\pi) = G_0(\nu) = G_0 = \frac{20}{A} \text{ MeV} \;,$$

$$\kappa_\pi = \kappa_\nu = \kappa_{\pi\nu} = \kappa = 140\, A^{-5/3} \text{ MeV fm}^{-4} \;, \tag{3.8}$$

$$G_2(\pi) = G_2(\nu) = G_2 = 0.71\ \kappa \;.$$

For calculating the Eλ transition densities we have used the effective charges

$$e^\pi_{\text{eff}} = 1.5\, e \;, \quad e^\nu_{\text{eff}} = 0.5\, e \;, \tag{3.9}$$

where e is the "bare" charge of a proton. The above parameters except G_0 and e^ρ_{eff} are rather similar to those employed by TTT [ref. 3)].

3.2. LOW-ENERGY SPECTRA AND E2 TRANSITIONS

The calculated excitation energies of the lowest 2^+ and 4^+ states [eq. (2.30) with ω = GS, J=2,4] are shown (as full lines) in figs. 1 and 2, respectively. For comparison, we also display the experimental values[19] (circles), the TTT results

of ref.[3] (dotted lines) and the phenomenological IBM results[14] (dashed lines) . As is seen from the figure, our results exhibit a more systematic behaviour and they provide a better explanation of experimental data in the region A $\geq$ 150 than the results of TTT. A good agreement of our results with the phenomenological IBM also indicates that the present approach may have certain relevance with respect to the microscopic foundation of the IBM. The most interesting observation, however, is the fact that, unlike TTT, we are able to reproduce the phase transition at A = 150-152 quite nicely. This is seen very clearly from fig.3, where the ratio $E(4_1^+)/E(2_1^+)$ is drawn.

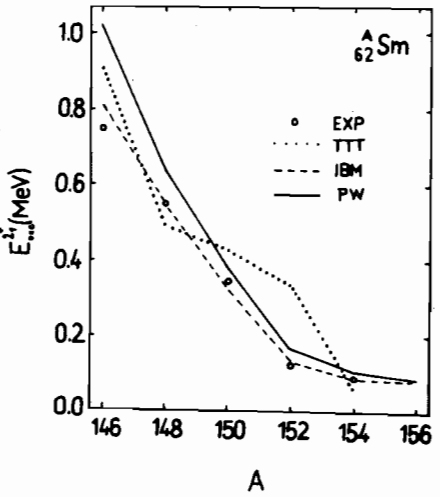

Fig.1. Excitation energies of the 2_1^+-states in $^{146-156}$Sm. The solid line connects the values calculated in the present work (PW) according to eq.(2.30) with ω = GS and J=2. The single-particle space and the nucleon-nucleon interaction are described in subsect. 3.1. The results are compared with: (a) the experimental data (circles - ref.[29]); (b) the IBM results (dashed line - ref.[14]); (c) the results of Thorn, Tsukuma and Takada (TTT) (dotted line - ref.[3]).

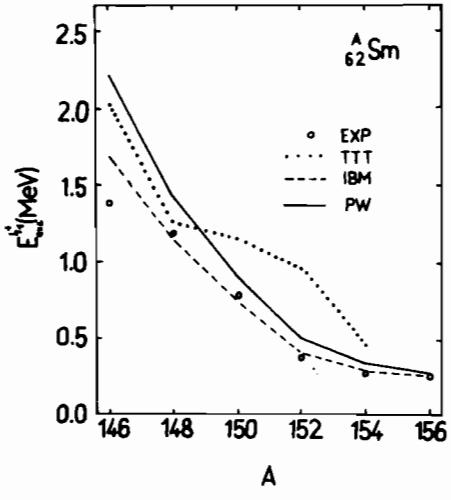

Fig.2. The same as in fig.1 for the 4_1^+-states.

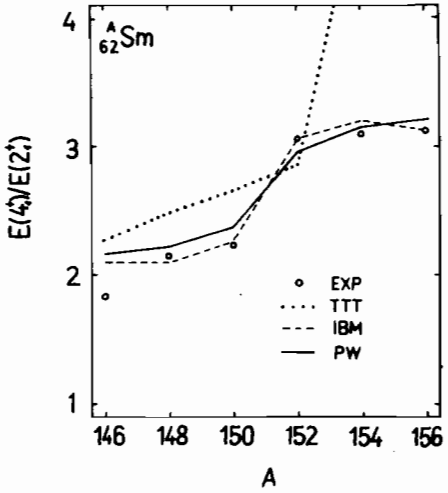

Fig.3. The ratio $E(4_1^+)/E(2_1^+)$ calculated with the values displayed in figs 1 and 2.

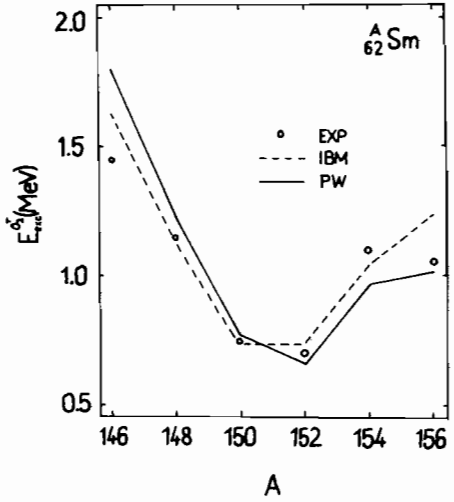

Fig.4. Excitation energies of the 0_2^+ states in $^{146-156}$Sm. The results of the present work (PW - solid line) are obtained using eq.(2.30) with ω = i = 1 [see (2.24)] and J=0. The experimental values[29] and the IBM results[14] are shown for comparison.

In order to see whether these results are not accidental, we have also calculated other quantities that exhibit characteristic changes during the transition from the spherical to the deformed region. In fig. 4 we show the excitation energies of the second (the first excited) 0^+ state calculated according to eq. (2.30) with ω = i = 1 and J=0. The results (solid line) are seen to reproduce the qualitative behaviour of experimental data quite well. Unfortunately, TTT have not reported the results of their

approach for the 0^+_2 states, and therefore, we compare our results only with those of the phenomenological IBM [14]. As is well known, the phase transition in $^{150-152}$Sm manifests itself as a sharp enhancement of the $B(E2; 0^+_1 \to 2^+_1)$ rate. The respective values calculated using eqs. (2.31) - (2.33) are shown in fig. 5. They reproduce the experimental data remarkably well and they are fully comparable with the IBM results. Even a more stringent test of our approach is provided by the $0^+_1 \to 2^+_1$ transition densities, calculated according to eq. (2.32) and displayed in fig. 6.

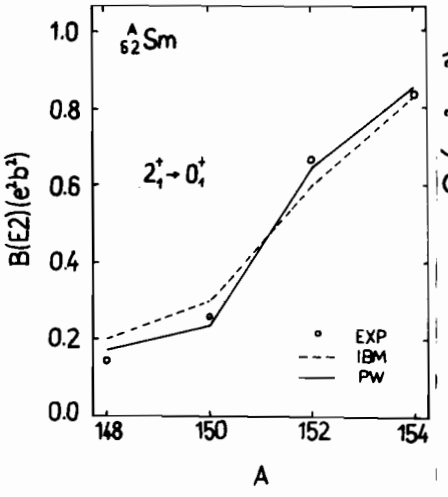

Fig.5. $B(E2; 2^+_1 \to 0^+_1)$ values around the "phase transition" region (A = 148 - 154) in the Sm isotopes. The results obtained in the present work (PW - solid line) according to eqs.(2.31) - (2.33) are compared with the experimental data [ref.[31]] and the IBM results [ref.[14]].

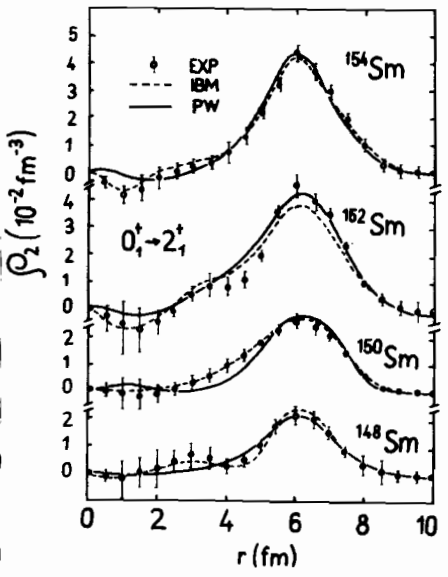

Fig.6. Radial densities for the $0^+_1 \to 2^+_1$ E2 transitions in $^{148-154}$Sm. The solid curves give our results obtained using eqs.(2.31) and (2.32). The experimental data were taken from ref.[32] and the IBM results (dashed curves) are from ref.[33].

Comparison with experimental data and the IBM results is very encouraging in favour of the present microscopic method. In particular, it is worth noticing that the "peak" value in ^{152}Sm is reproduced better than in the framework of the IBM.

3.3. THE ROLE OF BOSONS WITH DIFFERENT ANGULAR MOMENTA

As is shown in the preceding subsection, we have succeeded in reproducing the sudden phase transition associated with the change of nuclear shape in the Sm isotopes. On the other hand, TTT have failed in doing the same. Therefore, a natural question arises, what is the principal difference between the two approaches. An answer to the question can be found in the structure of the wave functions. In the table we show the quantities $|u^{\sigma}_{J\alpha}(\rho)|^2$, $\rho = \pi, \nu$ [see eqs. (2.27), (2.28)], which give the probabilities of finding the σ-th boson with angular momentum J in the GS condensate (2.15). It is seen from the table that the angular momentum structure of the boson condensate changes considerably with the varying mass number. While for A = 146 - 150 the GS bosons $B^+_0(\pi)$, $B^+_0(\nu)$ are dominated by the J=0 (s) and J=2 (d) components with an increasing relative importance of the latter, there is a noticeable increase in the percentage (from ~10% to roughly 30%) of the higher-multipole ($J \geq 4$) bosons for A $\geq$ 152. Especially the J=4 (g) bosons appear to be the most important ones. However, since the amount of a particular boson with given J in the mean-field condensate is generally considered to be a poor measure of its dynamical role in the description of physical observables [30], we have calculated the ratio $E(4^+_1)/E(2^+_1)$ and the $B(E2; 0^+_1 \to 2^+_1)$ values in two approximations in which the angular momentum structure of the GS wave function is restricted to contain only s,d and s,d,g bosons, respectively. The results are displayed in fig. 7 and they clearly show that for a correct reproduction of the phase transition

TABLE

The structure of the Hartree bosons $B^{+}_{0}(\pi), B^{+}_{0}(\nu)$*

	J	σ		^{146}Sm	^{148}Sm	^{150}Sm	^{152}Sm	^{154}Sm	^{156}Sm
$\lvert \mathcal{U}^{0}_{J\sigma}(\pi) \rvert^2$	0	0	s	0.542	0.384	0.239	0.152	0.150	0.128
	0	1		0.135	0.097	0.094	0.081	0.073	0.069
	0	2		0.026	0.023	0.022	0.042	0.042	0.045
	2	0	d	0.147	0.241	0.346	0.216	0.245	0.251
	2	1		0.031	0.085	0.100	0.102	0.117	0.123
	2	2		0.022	0.030	0.041	0.063	0.082	0.086
	2	3		0.001	0.005	0.007	0.037	0.040	0.043
	4	0	g	0.045	0.051	0.060	0.187	0.165	0.160
	4	1		0.011	0.012	0.021	0.045	0.061	0.055
	4	2		0.004	0.005	0.007	0.020	0.022	0.029
	6	0		0.012	0.049	0.026	0.032	0.033	0.024
	6	1		0.009	0.010	0.015	0.030	0.011	0.010
	8	0		0.005	0.004	0.011	0.046	0.006	0.003
	10	0		0.001	0.001	0.002	0.005	0.002	0.001
$\lvert \mathcal{U}^{0}_{J\sigma}(\nu) \rvert^2$	0	0	s	0.621	0.437	0.296	0.123	0.111	0.107
	0	1		0.116	0.093	0.060	0.043	0.040	0.043
	0	2		0.034	0.027	0.025	0.040	0.042	0.020
	2	0	d	0.104	0.285	0.421	0.384	0.339	0.321
	2	1		0.032	0.048	0.053	0.071	0.103	0.099
	2	2		0.014	0.024	0.028	0.040	0.052	0.054
	2	3		0.002	0.007	0.009	0.029	0.033	0.034
	4	0	g	0.029	0.034	0.040	0.136	0.134	0.151
	4	1		0.010	0.011	0.014	0.015	0.019	0.018
	4	2		0.002	0.004	0.002	0.003	0.004	0.006
	6	0		0.018	0.015	0.018	0.031	0.040	0.051
	6	1		0.003	0.001	0.003	0.005	0.005	0.007
	8	0		0.009	0.009	0.012	0.025	0.031	0.040
	10	0		0.004	0.005	0.008	0.012	0.019	0.025
	12	0		0.001	0.002	0.009	0.010	0.010	0.010

*The probabilities $\lvert \mathcal{U}^{0}_{J\sigma}(\rho) \rvert^2 (\rho = \pi, \nu)$ of finding the $b^{+}_{J\sigma}(\rho)$-bosons of eq. (2.26) in the mean-field bosons $B^{+}_{0}(\rho)$, appearing in the ground state (2.15), are presented [see eqs. (2.27), (2.28)] . Not all the probabilities are given in detail. Many of them are close to zero and the sum of the probabilities not shown explicitly does not exceed 1%.

Fig.7. The ratio $E(4^{+}_{1})/E(2^{+}_{1})$ (upper part) and the $\mathcal{B}(E2; 2^{+}_{1} \to 0^{+}_{1})$ values (lower part) in $^{148-154}$Sm, calculated within the present method in different approximations for the angular momentum structure of the mean-field (MF) boson condensate (2.15). The solid lines are obtained in the case when the MF wave function is truncated so as to contain the J=0 (s), J=2 (d) and J=4 (g) bosons. The dash-dotted lines correspond to the truncation to s- and d-bosons only.

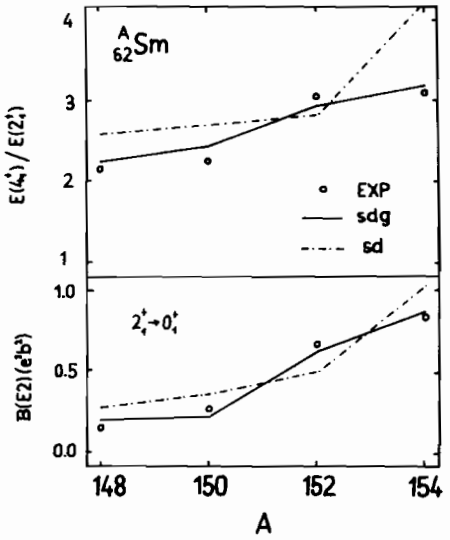

around A=150 - 152 the g- bosons are of crucial importance . It is just this point that we believe to be the main reason for the failure of the TTT approach where only the quadrupole (d) bosons were considered (the s- bosons being taken into account through the quasiparticle transformation) .

4. Summary and conclusions

In this paper, we have shown that a combined use of the Dyson boson mapping and the mean-field (MF) approximation is capable of describing the phase transition in the chain of Sm isotopes. In contrast to other approaches, the boson mapping has been applied directly to the shell-model hamiltonian without introducing the quasiparticle transformation. An appropriate physical boson subspace satisfying the Pauli principle has been selected by imposing a subsidiary constraint on the variational parameters in the MF boson wave functions. The rotational symmetry, which is broken in

the MF approach, has been restored through the angular momentum projection. In order to get an idea on the reliability of the present approach, we have calculated both the global characteristics, such as the low-energy spectra and B(E2) values, and the differential ones, namely the E2 transition densities. The results have been compared with those of the phenomenological IBM [ref. 4)] and those of the quasiparticle approach of TTT [ref. 3)] . We have also analyzed the angular momentum structure of the MF boson GS wave function and the role of different components in reproducing physical observables. The main conclusions from our investigation can be summarized as follows:

(i) The proposed method provides a satisfactory and unified microscopic description of the low-energy spectra, B(E2) values and E2 transition densities in the whole chain of even-even isotopes $^{146-156}$Sm, including the sudden phase transition from spherical to deformed shape in the region A = 150 - 152.

(ii) The results obtained within the present approach are comparable in quality with those resulting from the phenomenological IBM. At the same time, they are superior to the results obtained microscopically by TTT in ref. 3) .

(iii) Being free from the quasiparticle transformation, our method leads directly to a one- plus two- body hermitian boson hamiltonian, thereby avoiding the necessity of a hermitization procedure. For the same reason, the present method does not involve the problem of identifying and removing the spurious states associated with the particle number non-conservation.

(iv) We have found that the bosons with angular momentum J=4 (g-bosons) play a crucial role in the adequate description of the phase transition in the Sm isotopes. This fact can probably be identified as the origin of the failure of the TTT approach, where only quadrupole (J=2) bosons were considered.

References

1) A.Arima and F.Iachello, in Advances in Nuclear Physics, vol.13, ed. J.W.Negele, (Plenum, NY, 1984) , and references therein

2) T.Kishimoto and T.Tamura, Nucl.Phys.A270 (1976) 317

3) H.Tsukuma, H.Thorn and K.Takada, Nucl.Phys.A466 (1987) 70

4) P.Ring and P.Schuck, The nuclear many-body problem (Springer, New York, 1980) , and references therein

5) T.Holstein and H.Primakoff, Phys.Rev.58 (1940) 1098

6) G.Holzwarth, D.Janssen and R.V.Jolos, Nucl.Phys.A261 (1976) 1 ; T.Tamura, K.Weeks and T.Kishimoto, Phys.Rev.C20 (1979) 307

7) F.J.W.Hahne, Phys.Rev.C23 (1981) 2305

8) F.J.Dyson, Phys.Rev.102 (1956) 1217

9) K.Takada, Nucl.Phys.A439 (1985) 489 ; K.Takada, T.Tamura and S.Tazaki, Phys.Rev.C31 (1985) 1948 ; K.Takada, Phys.Rev.C34 (1986) 750

10) K.Takada and S.Tazaki, Nucl.Phys.A448 (1986) 56 ; K.Takada and K.Yamada, Nucl.Phys.A462 (1987) 561

11) M.R.Zirnbauer, Nucl.Phys.A419 (1984) 241 ; W.Pannert and P.Ring, Nucl.Phys.A465 (1987) 379

12) M.C.Cambiaggio and J.Dukelsky, Phys.Lett.197B (1987) 479

13) D.R.Bes, R.A.Broglia, E.Maglione and A.Vitturi, Phys.Rev.Lett.48 (1982) 1001 ; N.Yoshinaga, A.Arima and T.Otsuka, Phys.Lett.143B (1984) 5 ; T.D.Cohen, Nucl.Phys.A436 (1985) 165 ; W.Pannert, P.Ring and Y.K.Gambhir, Nucl.Phys.A443 (1985) 189

14) O.Scholten, F.Iachello and A.Arima, Ann.Phys.(N.Y.) 115 (1978) 325

15) B.R.Barrett, Rev.Mexicana de Fis. 27 (1981) 533 ; A.Arima and F.Iachello, Ann.Rev.Nucl.Part.Sci (1981) 75

16) E.R.Marshalek, Nucl.Phys.A224 (1974) 221 ; V.G.Pedrocchi and T.Tamura, Phys.Rev.C28 (1983) 410 ;

H.B.Geyer, C.A.Engelbrecht and F.J.W.Hahne, Phys.Rev.C33(1986) 1041

17) D.Janssen, F.Dönau, S.Frauendorf and R.V.Jolos, Nucl.Phys. A172(1971)145

18) J.A.Sheikh, Phys.Rev.C36(1987)848

19) H.B.Geyer and S.Y.Lee, Phys.Rev.C26(1982)642

20) P.Park, Phys.Rev.C35(1987)807

21) C.T.Li, Phys.Rev.C29(1984)2309

22) S.Pittel, P.D.Duval and B.R.Barrett, Ann.Phys.144(1982)168; A.van Egmond and K.Allaart, Nucl.Phys.A425(1984)274; J.Dukelsky, S.Pittel, H.M.Sofia and C.Lima, Nucl.Phys. A456(1986)75

23) S.Pittel and J.Dukelsky, Phys.Lett.128B(1983)9; F.Catara, A.Insolia, E.Maglione and A.Vitturi, Phys.Rev. C29(1984)1916

24) J.Dukelsky et al., Phys.Lett.129B(1983)1 Phys.Lett.130B(1983) 123; Nucl.Phys.A425(1984)93; Phys.Lett.144B(1984)145; Phys.Rev.C32(1985)335

25) J.A.Sheikh and Y.K.Gambhir, Phys.Rev.C34(1986)2344

26) H.Überall, Electron Scattering from Complex Nuclei (Academic, New York, 1971); T.W.Donnelly and J.D.Walecka, Ann.Rev.Nucl.Sci 25(1975)329

27) A.L.Steshenko, Nucl.Phys.A445(1985)462 P.Park and J.P.Elliott, Nucl.Phys.A448(1986)381 P.Czerski et al., Nucl.Phys.A465(1987)189 M.G.Vassanji and D.J.Rowe, Nucl.Phys.A466(1987)227 A.E.L.Dieperink and E.Moya de Guerra, Phys.Lett.189B(1987)267

28) R.A.Uher and R.A.Sorensen, Nucl.Phys. 86(1966)1

29) M.Sakai and A.C.Rester, Atomic and Nuclear Data Tables 20 (1977)441

30) E.Maglione, A.Vitturi, C.H.Dasso and R.A.Broglia, Nucl.Phys.A404(1983)333; T.D.Cohen, Nucl.Phys.A436(1985)165

31) R.M.Diamond et al., Phys.Rev.C3(1971)344; Nucl.Phys.A184 (1972)481; N.Rud et al., Nucl.Phys.A191(1972)545

32) M.A.Moinester et al., Phys.Rev.C24(1981)80

33) M.A.Moinester, J.Alster, G.Azuelos and A.E.L.Dieperink, Nucl.Phys.A383(1982)264

Received by Publishing Department
on Maroh 4, 1988.